

A comparison of the optical properties of radio-loud and radio-quiet quasars

P. Goldschmidt

Imperial College of Science Technology and Medicine, Blackett Laboratory, Prince Consort Road, London, SW7 2BZ, UK, p.goldschmidt@ic.ac.uk

M. J. Kukula

Space Telescope Science Institute, 3700 San Martin Drive, Baltimore, MD 21218, USA and
Institute for Astronomy, University of Edinburgh, Royal Observatory, Blackford Hill, Edinburgh
EH9 3HJ, UK, kukula@stsci.edu

L. Miller

Nuclear and Astrophysics Laboratory, University of Oxford, Keble Road, Oxford, OX1 3RH, UK,
l.miller1@physics.oxford.ac.uk

and

J. S. Dunlop

Institute for Astronomy, University of Edinburgh, Royal Observatory, Blackford Hill, Edinburgh,
EH9 3HJ, UK, jsd@roe.ac.uk

ABSTRACT

We have made radio observations of 87 optically selected quasars at 5 GHz with the VLA in order to measure the radio power for these objects and hence determine how the fraction of radio-loud quasars varies with redshift and optical luminosity. The sample has been selected from the recently completed Edinburgh Quasar Survey and covers a redshift range of $0.3 \leq z \leq 1.5$ and an optical absolute magnitude range of $-26.5 \leq M_B \leq -23.5$ ($h, q_0 = 1/2$). We have also matched up other existing surveys with the FIRST and NVSS radio catalogues and combined these data so that the optical luminosity-redshift plane is now far better sampled than previously. We have fitted a model to the probability of a quasar being radio-loud as a function of absolute magnitude and redshift and from this model infer the radio-loud and radio-quiet optical luminosity functions. The radio-loud optical luminosity function is featureless and flatter than the radio-quiet one. It evolves at a marginally slower rate if quasars evolve by density evolution, but the difference in the rate of evolutions of the two different classes is much less than was previously thought. We show, using Monte-Carlo simulations, that the *observed* difference in the shape of the optical luminosity functions can be partly accounted for by Doppler boosting of the optical continuum of the radio-loud quasars and explain how this can be tested in the future.

Subject headings: quasars, radio properties, evolution

1. Introduction

Quasars were first discovered at radio frequencies (Schmidt, 1963, Hazard, Mackay & Shimmins 1963) but subsequently only a small percentage were shown to emit a significant fraction of their bolometric power in the radio (Sandage, 1965). The distribution of radio luminosities appears to be bimodal as shown by Miller, Peacock & Mead, 1990, (hereafter MPM) Stocke et al. (1992) and Hooper et al. (hereafter HIFH, 1995). It is this observation which has prompted many workers to classify quasars as being ‘radio-loud’ or ‘radio-quiet’. The usual division between the two classes is taken to be $\log 10(P_{5GHz}(\text{W/Hz/ster})) = 24$ which is the value that we have adopted in this paper (we also assume $q_0 = 0.5$, $h = 0.5$, $\Lambda = 0$ throughout unless specifically stated otherwise). The results in this paper are not too dependent upon the exact value of this dividing line although we discuss below how they are affected by different definitions of radio-loudness.

However, not all workers use radio luminosity to define radio-loudness; Kellermann et al. (1989) used R , the ratio of radio to optical luminosity. This is a physically meaningful parameter only if radio and optical luminosities are *linearly* correlated. Peacock et al. (1986) and MPM argue that this cannot be so, otherwise the fraction of optically faint radio-louds should be much higher than measured. No linear correlation has been observed, at least for radio-loud quasars (Stocke et al., 1993) although this might be dependent on spectral index as Serjeant et al. (1997) claim a non-linear correlation in their large sample of steep-spectrum quasars.

The debate over how to define radio-loudness is indicative of the fact that we do not understand the link between radio and optical emission of quasars. It is still not known what the likelihood of a quasar being radio-loud is as a function of optical luminosity and redshift. The Palomar-Green Bright Quasar Survey (BQS, Schmidt & Green, 1983) is the most studied sample of optically selected quasars at radio wavelengths and the only one in which the sensitivity allowed the detection of some radio-quiet quasars (Kellermann et al., 1989) but even so, these data cannot distinguish between the two opposing hypotheses in which the radio output is either independent of optical luminosity or is correlated with it.

MPM used the BQS radio data together with VLA observations of higher redshift quasars to show that the fraction of radio-louds increased as redshift decreased. More recently La Franca et al. (1994), using a compilation of several radio studies, also showed that the likelihood of a quasar being radio-loud increased as redshift decreased, but only if the BQS data were included. Without these data, there is little evidence for evolution in the fraction of radio-louds. Both MPM and La Franca et al. (1994) argue that the change in fraction of radio-louds with redshift implies that the radio-loud population evolve more slowly than the population as a whole. This could be an indication that the evolution is linked to the environments of these objects. Ellingson, Yee & Green (1991) have shown that radio-louds reside in much richer environments than radio-quiets. If the former evolve slower than the latter then perhaps this is because of an increased likelihood of the RLQs’ fuel supplies being ‘replenished’ in rich environments. However an alternative explanation is that inverse Compton scattering occurs in the lobes of RLQs at high redshift, thus

decreasing these objects' radio luminosities. If there were a correlation between radio and optical output then the optical evolution of RLQs would be measured to be lower than that of RQQs.

HIFH used VLA observations of one third of the Large Bright Quasar Survey (LBQS, Hewett, Foltz & Chaffee, 1995) and found that the number of radio-loud quasars does not increase as redshift decreases, in direct contrast to results using the BQS sample. However, by using only the LBQS, with the advantage of avoiding the usual mixture of different surveys with different (usually undetermined) selection effects, this paper suffered from the corresponding disadvantage of only spanning about 1 magnitude in luminosity at each redshift.

It has been shown that the BQS quasar survey is incomplete (Goldschmidt et al., 1992) by a factor of 3. Miller et al. (1993) have suggested that this incompleteness is *not* random with respect to radio properties, implying that the measured fraction of radio-louds in this sample is biased and cannot be used to determine the radio-loud optical luminosity function.

In this paper we use new radio observations of the optically-selected Edinburgh Quasar Survey, and analyse these along with existing data to quantify the relative numbers of radio-loud and radio-quiet quasars (RLQs and RQQs) in optically-selected samples as a function of optical luminosity and redshift. Our new data nearly doubles the number of known RLQs derived from optical quasar surveys. Figs. 1 and 2 show the coverage of the optical luminosity-redshift plane before and after the addition of the radio data described in this paper, while Fig. 3 shows the distribution of RLQs and RQQs in these samples. It can be seen that the new data not only increase the number of known radio-loud quasars selected from optical surveys but also samples far more of the optical luminosity-redshift plane, allowing us to disentangle the dependency of radio properties on both optical luminosity and redshift. The new data in Figs. 2 and 3 comprise 50 quasars from the Edinburgh Survey (Miller et al. 1998, in preparation), 76 from the AAT Survey (Boyle et al., 1988) and 222 from the LBQS (Hewett, Foltz & Chaffee, 1995).

This paper is set out as follows. Section 2 describes the quasar sample which was observed on the VLA, and the resulting data. Section 3 describes how part of the AAT quasar survey (Boyle et al., 1988) and LBQS were matched up with the NVSS and FIRST 1.4 GHz surveys respectively, and presents the resulting datasets. Section 4 discusses and quantifies evidence for bimodality in the radio luminosity distributions. Section 5 quantifies the likelihood of a quasar being radio-loud as a function of optical luminosity and redshift using maximum likelihood. It also presents results from a Monte-Carlo simulation of the properties of radio-louds. Section 6 discusses the implications of this model fitting and Section 7 summarizes the main conclusions of our work.

2. The current sample

A sample of 87 quasars were chosen at random from the recently completed Edinburgh Survey (Goldschmidt 1993, Miller et al. 1998, in prep.). The redshift distribution spans $0.3 \leq z \leq 1.5$. The objects chosen all have optical magnitudes less than $B_J = 18.2$.

2.1. Observations and data reduction

6-cm continuum observations were made using the Very Large Array (VLA) in the hybrid DnC configuration in 1993 December and 1994 January. A dual-IF observing mode was used with two 50-MHz bands centred on 4.8226 and 4.8726 GHz. Frequent observations of nearby point sources were used to phase calibrate the target sources. Each quasar was observed at two different hour angles in order to maximise coverage of the *uv*-plane, with a total on-source integration time of approximately 4 minutes per object.

We followed the standard calibration procedure within the AIPS package. Flux densities were calibrated relative to 3C286 (1328 + 307), using the revised coefficients from the 1990 VLA Calibrator Manual and leading to uncertainties in the derived fluxes of around 5%. The two IFs were combined to give an effective bandwidth of 100 MHz centred on 4.8476 GHz. The Fourier Transform was carried out using a natural weighting scheme to maximise the sensitivity in the final maps, giving a 3-sigma noise of roughly $0.2 \text{ mJy beam}^{-1}$.

The synthesized beam of DnC-array at 6 cm is $\sim 14''$ (FWHM) and the useful field of view (FOV) is $9'$ (the primary beam of the individual array elements causes severe attenuation outside this region). Because of this large effective FOV many field sources appeared in the final maps. We rejected as field sources any detections which were more than $14''$ from the optical position of the quasar (at the lowest redshift of the sample this would correspond to a projected linear distance of 80 kpc), leaving us with 16 radio detections and 71 upper limits.

The shortest baseline in this configuration is 35 m so the array will only become ‘blind’ to featureless extended emission on scales larger than $5'$ which is much larger than any structures likely to be associated with quasars in our redshift range.

2.2. Results

The results of the observations are detailed in Table 1. For objects with a radio detection we give the measured flux and position of the radio source, obtained by fitting a two-dimensional Gaussian function with the AIPS task JMFIT. We estimate that the radio positions are accurate to $\sim 0.1''$. For the brighter sources the uncertainty in the flux measurement is dominated by the $\sim 5\%$ calibration uncertainty; for weaker objects the 3-sigma noise of $\sim 0.2 \text{ mJy beam}^{-1}$ dominates. Eight quasars in the Edinburgh sample were already known to be Parkes, Molonglo, Green Bank or Texas radio sources (these are indicated in the table) and for these objects the fluxes in this paper are in very good agreement with the previous measurements for those quasars measured at the same frequency.

Also, 37 of our objects are in common with the LBQS and have been observed by HIFH, we have also included their determinations of the 8.4 GHz fluxes in the table, and spectral indices where relevant. The mean spectral index for the few objects detected by both HIFH, and us is 1,

and the variance is large.

For non-detections we quote the optical position of the quasar and an upper limit on the radio flux based on the 3-sigma noise measured over the central part of the map.

Even with the rather coarse angular resolution of the DnC-configuration, three quasars, 1303+020 1407-023, and 1430-004, showed evidence for extended radio structure in the form of double or triple sources straddling the optical nucleus (the high degree of symmetry exhibited in each case makes it extremely unlikely that these structures are merely due to a fortuitous alignment of background sources). For 1430-004 we took the flux of the central component as the flux of the object.

3. Matching existing optical quasar catalogues with recent radio surveys

There have been two major radio surveys carried out in the past few years, the NRAO VLA Sky Survey (NVSS; Condon et al., 1998) and FIRST (White et al., 1997), that are capable of detecting all known radio-loud quasars out to $z \sim 2$. FIRST is in fact so sensitive (rms noise is ~ 0.15 mJy) that it can detect many low- z radio-quiet quasars. In the next two subsections we describe matching up these surveys with the AAT and the LBQS surveys respectively to increase the statistics and also the coverage of the $L - z$ plane.

3.1. Matching the AAT survey with NVSS data

The AAT quasar survey (Boyle et al., 1988) has an optical flux limit of $B \leq 21$, over 2 magnitudes fainter than the Edinburgh survey or LBQS. No radio data are available for the AAT quasar survey. We therefore attempted to match up this survey with the NVSS to find radio detections associated with the quasars.

The NVSS has a typical noise of $1\sigma = 0.45$ mJy/beam and the available catalogue is complete to a flux limit of 2.4 mJy. This means that the survey can detect all known radio-loud quasars with $z \leq 1.5$ if they have luminosities $\log 10(P) \geq 24$. This is supported by Bischof & Becker's recent (1997) matchup of the NVSS catalogue with the Véron-Cetty & Véron quasar catalogue from which they conclude that the NVSS can detect most known radio-loud quasars.

A radio detection in the NVSS was deemed to be an AAT quasar if it lay within a 30 arcsecond radius around the optical position. There are 191 sources in the AAT sample within the NVSS area. Of these, 76 are quasars with $0.3 < z < 1.5$ and $M_B \leq -23$ so we consider this subset to be a 'complete' catalogue at both optical and radio wavelengths. Using the criteria outlined above we matched up 5 of these 76 quasars with NVSS detections. Although 30 arcseconds is rather a large radius to use, the surface density of sources in the NVSS ($\sim 60 \text{ deg}^{-2}$) means that the probability of a random NVSS source being identified as the radio counterpart to the optical ID is 0.012 and

thus we expect that 1 out of our 76 quasars is spuriously matched up. In fact, 4 out of the 5 matched quasars have an offset between the optical and radio positions of < 5 arcseconds and one has an offset of 29 arcseconds. It therefore seems likely that this last source has been spuriously matched and we do not use its associated radio flux in the next sections. The coordinates, optical and radio flux densities of the 4 reliably identified quasars are given in Table 2.

Two of the above quasars are radio-loud, given our criterion. This is a very low fraction indeed (3%), which, if genuine, has important ramifications for the estimate of the radio-loud optical luminosity function (OLF). We will discuss this in more detail in the following sections. Bischof & Becker (1997) match up the first 2 of the quasars in the above table (their catalogue only goes up to 21h30), and do not match up any of the other AAT quasars. One of the detections is a known radio-loud quasar, PKS 2203-18.

Is the low number of associations a consequence of errors in either or both of the optical and radio positions? Condon et al. (1998) estimate the error in the position of a faint NVSS source as being ~ 5 arcseconds. The error in the optical positions is ~ 1 arcsecond (Boyle et al., 1988). Therefore given the large search radius, errors in the positions should not have affected the associations. Also, very sensitive radio observations of the very faint survey ($b \leq 22$, Zitelli et al., 1992) find 2 radio-loud quasars out of 55 (Gruppioni, private communication) which confirms the low fraction of radio-louds in the AAT survey.

We visually checked the associations by plotting NVSS fields for all the AAT quasars within the NVSS area and overlaying the optical positions. These visual searches confirmed the results above.

3.2. Matching the LBQS with the FIRST radio survey

In a similar manner we endeavoured to match the 1.4 GHz FIRST survey (White et al., 1997) with the LBQS. FIRST covers a smaller area to a deeper flux limit than the NVSS; the 1σ noise is on average 0.15 mJy, and the available catalogue is complete to 1 mJy. Therefore we estimate it should be capable of detecting radio-loud quasars out to $z \geq 2.2$. HIFH and Visnovsky et al. (1993) present VLA measurements of 1/3 of the quasars in the LBQS, however as HIFH show, the quasars chosen for the VLA observations are more luminous and at higher redshifts than the quasars not observed. Therefore by matching up the LBQS with FIRST we should be able to extend coverage of the L-z plane to slightly fainter luminosities, as well as improving the statistics.

The average surface density of the sources in the FIRST is 90/degree², and we chose a 10 arcsec radius around each LBQS position within which to search for coincident radio sources. The likelihood of a random radio source being matched up with the LBQS quasar is 2.2×10^{-3} . There are 222 LBQS quasars within the FIRST survey area so we therefore expect 0.5 spurious matches.

We found a total of 28 detections out of the 222 quasars (Table 3). Two of these are known

to be Parkes sources; PKS 0256-005 and PKS 0056-00. Radio fluxes for 34 of these objects have already been reported in HIFH. Of these 34 objects, 4 are detected by both FIRST and HIFH, 1 object is undetected by HIFH but FIRST detects it, and 2 objects are detected by HIFH and not by FIRST. These latter objects are radio-loud but at $z = 3.281$ and $z = 3.015$ and therefore their radio luminosities are just below the flux limit of FIRST (depending upon our assumed spectral index), *i.e.* we expect FIRST to be incomplete at these high redshifts. The rest of the 27 quasars in common are undetected by both surveys. This comparison indicates that the low number of radio-loud quasars that we find in the LBQS-FIRST match-up is genuine and not due to incompleteness in FIRST.

Many of our FIRST associations are in fact low redshift radio-quiet quasars and the fraction of radio-louds is slightly lower than in HIFH who estimate that 10% (27 out of 256) of their quasars are radio-loud, whereas we estimate that 7.7% (17 out of 222) of ours are radio-loud. The difference is not statistically significant. However it could be due to the fact that the LBQS quasars that we have matched up are on average fainter and at higher redshifts than the sample in Hooper et al, as shown in Fig. 2.

3.3. Coverage of the optical luminosity-redshift plane

Here we briefly summarize the main properties of the samples used in this paper.

Fig. 2 shows the coverage of the optical luminosity - redshift plane achieved to date in published radio surveys of optically-selected quasars, together with the data discussed in Sections 2 and 3.1 and 3.2 above. We do not include the BQS survey on this figure because of the doubts mentioned above about the possible bias in this survey towards radio-loud quasars; this is discussed in more detail in Section 5.1. The plot highlights the problem of the luminosity-redshift correlation which is endemic in flux-limited surveys, with the result that large regions of the plane remain unsampled. This patchy coverage is of particular concern in studies such as the current one, in which we wish to separate the effects of redshift and absolute magnitude on quasar radio properties. In order to do this with any degree of confidence we need to be able to compare objects of similar absolute magnitude at different redshifts and vice versa. It can be seen that the MPM data breaks this luminosity-redshift degeneracy at $z \sim 2$ and now, using the combined data from AAT, LBQS and Edinburgh we can break the degeneracy at lower z as well.

The LBQS, although by far the largest sample to have been surveyed in the radio is not ideally suited to this purpose when considered in isolation; for a particular redshift the spread in absolute magnitude amounts to only a magnitude or so (Figure 1) making it impossible to compare objects of equivalent optical luminosity over redshift intervals of $z \geq 0.2$. However this is a very large sample; 359 LBQS quasars were observed with the VLA by Hooper et al. (1994, 1995) and Visnovsky et al. (1993) with $0.2 < z < 3.4$ and $-23 > M_B > -28$.

The samples of MPM consist of 105 quasars and provides fairly uniform coverage of the region

$1.8 < z < 2.4$ and $-25 > M_B > -27.5$. MPM used the VLA in C-configuration at 5 GHz (6 cm; 5-arcsec resolution) to observe 99 quasars from the quasar surveys of Osmer (1980) and Osmer & Smith (1980), and included a further 6 quasars from Smith & Wright (1980). With typical 3σ sensitivities of ~ 0.6 mJy beam $^{-1}$, this corresponds to a radio luminosity of $10^{24} \text{W Hz}^{-1} \text{ster}^{-1}$.

Schneider et al. (1992) present radio data for 22 quasars at high redshift ($3.2 < z < 4.7$), covering a similar range of absolute magnitudes ($-25.0 \geq M_B \geq -27.5$) to MPM.

La Franca et al. (1994) observed 23 optically selected quasars from the SA94 survey (La Franca et al., 1992) and detected 4 of them. They achieved a 1σ noise of ~ 0.05 mJy and find their data are consistent with a bimodal radio distribution out to moderately high redshifts.

It is extremely important to point out that many of the observations made by other authors and used for comparison in this paper were not carried out using the same wavelengths and magnitude systems. For the purposes of Figs. 2 and 3, and in all subsequent discussion, we have transformed the original data to our preferred units: radio flux density at a rest wavelength (after k -corrections) of 6 cm (5 GHz) and absolute magnitudes measured in the B Johnson system. The assumptions made during this process have important implications, and merit some discussion. Because Figs. 2 and 3 cover a large range of redshifts and because not all of the quoted radio observations were carried out at a wavelength of 6 cm (5 GHz), the assumed form of the quasar spectrum is doubly important as it affects both the transformation from one *observed* wavelength to another and the transformation to the same *rest* wavelength in each case. For the purposes of k -corrections and the transformation of radio flux density between different observing bands we take the optical and radio spectral slopes to be α_O and $\alpha_R = 0.5$, where flux density $S_\nu \propto \nu^{-\alpha}$. The few objects for which we possess spectral information have rather flat spectra with $\alpha \leq 0.5$ (see above) but the scatter is large and therefore the data are reasonably consistent with this assumption and do not justify the use of a different value. However, we note that a significantly steeper or flatter spectrum might conceivably affect the fraction of objects classified as radio loud or radio quiet, or raise the effective luminosity limit of a survey to a level at which it is impossible to distinguish between radio-loud and radio-quiet using the criterion described above.

For the optical luminosities we used M_B where B refers to the Johnson system. This is not the natural system for most of the quasar samples discussed above and hence we transformed the apparent B_J magnitudes in the Edinburgh survey assuming the transformations in Blair & Gilmore (1982) and a mean $B_J - V$ colour of 0.18 to give $B = B_J + 0.06$. For the AAT survey we used the transformation given in Boyle et al. (1988); $B = b - 0.1$. For the LBQS quasars we used the absolute magnitudes given in HIFH which are transformed to the B system. For the LBQS quasars in the FIRST survey we used the same transformation as for the Edinburgh quasars. The MPM quasars already have apparent magnitudes quoted at the rest-frame wavelength of 1475 Å and thus we transform them to B using $B = m_{MPM} + 0.23$ which is correct at the average redshift of the sample.

There are clear inconsistencies involved in transforming all these different surveys to a

common system. Ideally one would like to use the natural system without any transformation as this only increases the uncertainty. Also, an estimate of the *continuum* flux without any contribution from emission lines would be ideal, especially for this type of study, as it is possible that radio-louds and -quiets might have different emission line strengths. In spite of this caveat, the uncertainties involved in transforming from one system to another are most likely much smaller than the random errors in the measured fluxes which could be as high as 15%.

A comparison of Figs. 1, 2 and 3 show how the radio information on the AAT survey covers a part of the M_B -z plane that has not been sampled before. They also show how increasing the radio coverage of the LBQS improves the statistics of brighter quasars. Both these improvements allow us to determine the OLF of radio-louds over a wider range of redshifts. We do this below, in Section 5.

4. Evidence for bimodality in the radio luminosity distribution

Strittmatter et al. (1980) and MPM argued that the distribution of radio luminosities is bimodal. If true, this has important implications for our understanding of the origins of radio emission in quasars. In this section we look at how to test for bimodality and what conclusions can be drawn from the results. Figs. 4 and 5 show the optical and radio luminosity distributions for the data used in this paper separated into two redshift bins. It can be seen that there is some evidence for bimodality but this is not overwhelming, particularly at low redshift where there is little evidence for a ‘gap’ at $\log(P) \sim 24$.

It is not trivial to quantify the likelihood of a dataset being bimodal. One maximum-likelihood-based method is the Lee statistic (Lee, 1979, Fitchett, 1988). This looks at the variances in subsets of the data and compares the weighted sum of these variances with that for the whole dataset. If there is a way of dividing the data such that the variances in each subset are very much smaller than for the dataset as a whole then this implies that the distribution is bimodal. However to quantify the significance of this one needs to assume a parametric unimodal distribution and estimate (from Monte-Carlo simulations) the likelihood of the Lee statistic describing this as bimodal. Clearly the major problem is that most of the data consists of upper limits and hence we have little idea of what sort of parametric distribution to assume. A reasonable approach seems to be to use the upper limits as detections and fit a gaussian with a uniform tail to high radio luminosities. Stocke et al. (1992) and HIFH used similar approaches.

The Lee statistic was calculated in 2 redshift bins; $0.5 \leq z < 1.5$ and $1.5 \leq z \leq 2.5$. We then estimated the significance of the measured Lee ratios from Monte-Carlo simulations of a unimodal distribution consisting of a Gaussian with a uniform tail to high luminosities. In neither of the 2 redshift bins were the measured Lee ratios estimated to be significantly different from the distribution of Lee ratios that we derived from the Monte-Carlo realisations. We conclude that there is insufficient evidence to show that the radio luminosity distribution is indeed bimodal.

HIFH reach the same conclusion and emphasize the need for more data.

5. Luminosity and redshift distributions of radio-loud quasars

5.1. Does radio-loud fraction vary with redshift?

In this and the next section we attempt to separate out the effects of z and M_B upon the fraction of radio-loud quasars; $f(RL)$. By combining the current sample with the LBQS we obtain 124 quasars in the absolute magnitude interval $-25.5 \geq M_B \geq -26.5$, covering a redshift range of $\Delta z = 0.6$ centred on $z = 0.9$. These objects have the same range of optical luminosities as the high-redshift ($z \simeq 2$) sample of MPM (assuming $\Omega = 1$), allowing us to test for signs of evolution in the fraction of radio-loud sources between the two epochs. We did this by calculating the numbers of radio-loud and -quiet quasars in each of the two redshift bins and carrying out a contingency table analysis. The fraction of RLs is 18% at low z , dropping to 8% at higher z . However this is not statistically significant; $\chi^2 = 2.06$ with 1 degree of freedom, and thus the fraction of radio-loud quasars to total number of quasars in each bin is consistent at the 15% level.

We then included the VLA data on very high redshift quasars from Schneider et al. (1992), and fitted a simple parametric model to the fraction of radio-loud quasars, $f(RL)$, as a function of redshift. We chose to model the data as

$$\frac{n(RL)}{n(RQ) + n(RL)} = A(1 + z)^\gamma \quad (1)$$

where $\gamma = 0$ if the fraction stays constant with redshift. The best fit parameters are $\gamma = -2.16$ and $A = 0.75$ (see Figure 6 for more details), indicating a slight decrease in $f(RL)$ with increasing redshift. However a constant fraction of radio-loud quasars with redshift cannot be ruled out and is consistent with the data at the 16% level.

We have also plotted the estimated fraction of radio-louds at low redshift from the BQS sample within the same magnitude range on Figure 6. It can be seen that the BQS sample has a higher fraction of radio-louds, which is different from the model at the 99.8% level.

To summarize, although there are hints that $f(RL)$ increases as z decreases for all M_B within the z range $0.6 < z < 2.5$ this is not statistically significant in the narrow M_B range that we have chosen. A more direct approach is to try and determine the fraction of radio-louds as a function of M_B in different redshift slices and we do this in the next section.

5.2. Radio-loud fraction as function of optical luminosity

Because we have managed to increase coverage of the $M_B - z$ plane by using the NVSS and FIRST radio surveys, we can attempt to estimate the fraction of radio-loud quasars as a function

of absolute magnitude in redshift slices without being too troubled by the usual luminosity-redshift degeneracy.

We used a subset of the data from the Edinburgh, LBQS, AAT, SA94 and Schneider et al. samples in two redshift bins, and measured the number of radio-loud quasars as a function of magnitude in each bin. Fig. 7 shows this fraction for each bin together with the best-fit model, discussed below. The error bars show the 1σ errors, which were calculated using $\sigma^2(f) = f(1 - f)/N$ where f is the RLQ fraction and N is the number of quasars per bin.

Below we provide a more detailed analysis of these plots but here we point out the main features.

- (a) In each redshift bin the fraction of radio-louds increases with luminosity. This implies that the radio-loud OLF is slightly flatter than the total OLF for most luminosities.
- (b) There is considerable overlap in the luminosities sampled, and thus we can say that the fraction of radio-louds is marginally higher within the luminosity range $-26.5 < M_B < -24.5$ at lower redshifts.

Together, these two observations are consistent with a model in which the radio-loud OLF is flatter than the total OLF but evolves at the same rate, such that in a given M_B slice as z decreases the fraction of radio-louds increases, as marginally indicated by the data. However, the data also imply that the RL OLF cannot be much flatter than the total OLF because the rate of change with z is only marginal. Below we compare such a model to the data and discuss its implications.

5.3. Model fit to radio-loud optical luminosity function

We can use the data to fit models to the optical luminosity function of radio-louds (and -quiets). We chose to do this using maximum likelihood (ML). The main advantage of this method over χ^2 is that it does not require the data to be binned first (see Marshall et al. 1984 for a detailed description of using ML to estimate best-fit parameters of luminosity functions). We formulated the likelihood function in the following way, similar to that in La Franca et al. (1994), in which it is assumed that the total (RL+RQ) OLF is *a priori* well-determined and therefore one can use the *relative* numbers of RLs (as a function of optical luminosity and redshift) to estimate the RL OLF. This is rather different in spirit from the likelihood function of Marshall et al. (1984), which used the *absolute* probability of detecting a quasar. We cannot use that method directly as we have, on the whole, only incomplete information on the radio properties of each survey and hence cannot determine the absolute normalisation of the RL OLF without taking into account the total number of quasars that have been observed. If p is the probability of a quasar being radio-loud then we can formulate the likelihood function as

$$\mathcal{L} = \prod_{i=1}^{N_{RL}} p(M_B, z) \prod_{i=1}^{N_{RQ}} (1 - p(M_B, z)) \quad (2)$$

and we choose to model p as an arbitrary function of M_B and z ;

$$p(M_B, z)dM_B dz = (1+z)^C 10^{A+B(M_B-M^*)+D(M_B-M^*)^2} dM_B dz. \quad (3)$$

We have to make a choice on the parameterization of the total OLF. As has been discussed in recent papers (Hewett et al. 1993, Miller et al. 1994, Koehler et al. 1997, Goldschmidt & Miller, 1998) the Pure Luminosity Evolution (PLE) model (Marshall et al. 1984, Boyle et al. 1988) - in which the shape of the luminosity function remains invariant at all redshifts and in which the evolution is parameterised by the characteristic luminosity M_* increasing with redshift - has been shown to be a poor fit to the more recent bright quasar surveys. Although it is not clear how to parameterize the ‘current’ OLF, the above authors have all shown using 3 independent surveys that the shape of the OLF changes with redshift in that it is flatter at low z . At $z < 1$ the OLF is a featureless power law.

Hewett et al. (1993) present a parameterization of the OLF for all quasars (radio-loud and radio-quiet) which is based on the optically selected LBQS. This is a more arbitrary model than PLE and clearly cannot be interpreted as having any physical meaning. We combined our model fit to the fraction of RLQs with the Hewett et al. parameterization of the OLF to give the OLFs of RLQs and RQQs separately.

We achieved a satisfactory fit (a probability of 15% from χ^2) to the data with the following parameters, $A = 0.50 \pm 0.05$, $B = -0.56 \pm 0.02$, $C = -2.12 \pm 0.18$, $D = 0.06 \pm 0.01$, $M^* = -28 \pm 0.10$; see Fig. 7 for a comparison of the model and data in two redshift bins. The errors on the parameters were estimated assuming a χ^2 distribution for $\Delta(-2 \log \mathcal{L})$. From our estimate of $p(M_B, z)$ we can now derive the radio-loud luminosity function (since it is defined as $\Phi_{RL} = p\Phi_{total}$). We discuss this further in Section 6 below.

5.4. Does Doppler boosting affect the optical luminosities of radio-loud quasars?

Above we showed that the best-fit model to the RLQ OLF is one which is skewed to higher luminosities than that of RQQs. Here we discuss a possible physical mechanism for the difference in the optical luminosity distributions.

In the orientation-based unification scheme (OBUS) the observed differences between radio-loud quasars and radio galaxies can be explained in terms of the differences in viewing angle. According to the OBUS objects that are viewed at large angles to the jet axis have more obscured optical continua and broad line regions. Objects viewed at small angles to the jet axis offer an almost unobscured view of the central region and inner regions. These latter objects are also more likely to suffer from Doppler boosting of the emission in the jet. It is this Doppler-boosted jet emission that we are concerned with here.

We suggest that this Doppler boosting may also affect the *optical* emission and hence the optical luminosity distribution of RLQs. Given a jet speed $v = \beta c$ and corresponding γ , together with a viewing angle θ from the jet direction and intrinsic spectral index α , the effect upon the observed flux S_{obs} given the intrinsic flux S_{int} is;

$$M = \frac{S_{obs}}{S_{int}} = \left[\frac{1}{\gamma (1 - \beta \cos(\theta))} \right]^{3+\alpha}. \quad (4)$$

The effect upon the observed fraction of radio-louds is a convolution of the above distortion with the intrinsic luminosity distribution of radio-louds. We modelled this using a Monte-Carlo simulation, with the following assumptions;

- a) We assumed that roughly 10% of the observed continuum flux at optical wavelengths is due to synchrotron emission.
- b) The maximum boost factor allowable is 10, implying that the flux of the object is doubled. There needs to be an upper limit factor on the possible range of boost factors, otherwise the simulation might produce an excess of BL Lac objects, compared with our observations.
- c) We assumed a uniform distribution for the jet speed; $0.1 \leq \beta \leq 0.95$.
- d) We used, as the intrinsic RLQ OLF, the fit to the RQQ OLF. In the absence of beaming this implies that the fraction of RLQs is constant with M_B .
- e) The range of viewing angles is $0 \leq \theta \leq 45$ degrees.

Fig. 8 shows the results of this simulation. The fraction of RLQs is clearly a function of optical luminosity and we can understand this as being due to a combination of faint objects being beamed and appearing brighter, and due to the finite slope of the luminosity function. Although the fraction of RLQs does increase with luminosity in this simulation, the dependency of $f(RL)$ upon M_B is not so strong as in our data and thus we conclude that Doppler beaming may be responsible for part of the observed dependency of $f(RL)$ upon M_B but cannot account for all of it, as this would predict that all of the most optically luminous objects are blazars.

6. Discussion

Figure 9 shows the derived optical luminosity functions for both RLQs and RQQs over the luminosity ranges for which we have information on the radio classes, given the estimated probability of a quasar being radio-loud as derived in Section 6. It can be seen that the RLQ OLF appears to be flatter and hence skewed to higher luminosities than that for RQQs. We have already discussed a possible physical cause of this flattening in the previous section. The next obvious question to ask is do both OLFs evolve at similar rates? Unfortunately it is not easy to see how to answer this question, principally because, as we discussed above, the total OLF changes shape. Because of this there is no obvious ‘feature’ in the OLF that can be traced at different redshifts and hence there is no straightforward parameterization of the evolution. If we consider density evolution then the RLQs evolve more slowly than the RQQs, as marginally indicated by

the data in Section 5. Without more information on the lifetimes of the objects, or more physically detailed models of evolution, one cannot say anything more, apart from noting that the lack of evolution between $1.5 < z < 2$ shows up in *both* classes of objects. This is a clear indication that the *onset* of optical evolution is a universal phenomenon and not directly related to radio power, whereas the *subsequent* evolution may well be a function of radio power.

The Doppler boosting mechanism discussed above may be tested using both radio and optical data. Although, as argued previously, the effect upon individual quasar SEDs is likely to be rather small, overall we can compare the average SEDs of RLQs and RQQs provided that they are well matched in *observed* optical luminosity. The beaming hypothesis predicts that the emission lines of the RLQ SED will have smaller equivalent widths than those of RQQs because of the extra beamed optical continuum. Using the radio properties to test this hypothesis will require not only detections of the RQQs but also spectral indices, as the hypothesis predicts that the radio spectra of RQQs will be steeper than those of RLQs. Also, with the current data we have not been able to sub-divide the RLQs on the basis of their spectral indices, however, if we restricted ourselves to the steep-spectrum objects, we would expect a more similar optical luminosity distribution to the RQQs since beaming should not be observed for these objects. Serjeant et al. (1997) are addressing this with their sample of radio-selected steep spectrum quasars.

There are various other plausible causes for the difference in OLFs for the two radio classes. One obvious difference between the two classes is the difference in host galaxies. This subject has a contentious history, in that for a long time it was an article of faith in AGN studies that radio-loud AGN resided in elliptical hosts, and radio-quiet AGN resided in spiral hosts. The evidence for this comes from very low redshift studies of Seyferts and radio galaxies. However until recently the evidence that this dichotomy extended to higher optical luminosities and/or redshifts was totally lacking. The recent papers by McLeod & Rieke (1995) and Taylor et al (1996) using NIR imaging of $z \leq 0.4$ RQQs and RLQs shows that the distinction between the hosts breaks down. In particular Taylor et al. found that the fraction of RQQs in elliptical hosts increases with optical luminosity. McLeod & Rieke showed that there appeared to be a lower limit to the luminosities of the hosts which was linked to that of the resident quasar. How does this fit in with our studies of OLFs? The answer is linked to Peacock et al.'s (1986) original reason for the lack of optically faint RLQs. If RLQs at faint luminosities are more likely than RQQs to be in large, luminous ellipticals then there are *two* ways that they could be selected against in optical surveys. The first is because of morphology, optical surveys usually require that quasar candidates are not extended (because of the photometric calibration on Schmidt plates), and thus an optically faint quasar in a luminous host galaxy is more likely to be discriminated against than one in a smaller and/or fainter host galaxy. The second possibility is that early-type galaxies appear to be redder than late-types and thus the overall colour of the AGN-plus-host system may not be UVX enough to satisfy the selection criteria of the survey.

However, the *shape* of the dependency of radio-loud fraction on optical luminosity may not be fully consistent with the above picture, in that one would expect the effect of incompleteness due

to large red hosts to kick in at faint luminosities, whereas the fraction of RLQs remains roughly constant over a wide range of M_B and increases sharply only at the highest luminosities sampled.

The observed difference in the OLFs could also be due to an underlying correlation between radio and optical luminosities combined with our definition of radio-loud as being above a cut-off in radio luminosity. The putative correlation would then mean that the observed optical luminosities of the RLQs chosen in this way are skewed to high values and hence the OLF is observed to be flatter than the true distribution.

A separate but related question is; are RLQs responsible for the flattening of the total OLF seen at $z \leq 1$? As discussed above, recent studies of the OLF show that it flattens at low redshifts. This could in principle be entirely due to RLQs having a relatively high space density at low z , compared to the population as a whole. But the change in power-law index of the OLF means that the space density of $z \leq 1$ quasars is roughly a factor 3 higher than indicated by the uniform PLE model. For RLQs to be responsible for this they would have to make up the bulk of the population (at least 60%) at low redshifts and this is not what we find.

7. Conclusions

We have acquired radio data for optically selected quasars from 3 different surveys and thus extended coverage of the optical luminosity-redshift plane for radio-loud and -quiet quasars. These new data have weakened the degeneracy between luminosity and redshift and allowed us to model the optical luminosity functions and their evolutions for the two classes of quasar. We note that this study depends on the combination of several different quasar samples, all with different primary selection criteria and amounts of bias. The cumulative effect of these biases is almost impossible to quantify, but we stress that until much larger, optically-selected quasar samples become available this remains the only way of obtaining sufficient coverage of the $M_B - z$ plane. Our conclusions can be summarized as follows:

- (1) Radio luminosity distribution: In agreement with previous work, the distribution of radio luminosities gives the impression of being bimodal, but a unimodal distribution cannot be ruled out with any significance from the results of the maximum-likelihood based Lee test.
- (2) Radio-loud fraction: The fraction of radio-louds decreases with optical luminosity, but there is little evidence for strong evolution of this fraction with redshift.
- (3) Optical luminosity functions: It appears that, at a given redshift, the optical luminosity function for radio-loud quasars is skewed towards higher luminosities and is flatter than that for radio-quiets. The optical luminosity function for the latter shows a change in shape, similar to that seen in the total optical luminosity function, although more radio data is needed for the most optically luminous quasars in order to fully substantiate this. Monte-Carlo simulations of radio-loud quasars with the *same* intrinsic optical luminosity function as radio-quiets show that if

10% of the optical emission for RLQs is synchrotron emission from the jet, then Doppler beaming can be responsible for the some of the *observed* difference in optical luminosity functions for the two classes of object.

(4) Evolution of RLQs and RQQs: The space density of radio-loud quasars evolves more slowly than that of radio-quiets at a given optical luminosity, although the evolution for both class of quasar slows similarly at $z \sim 2$. What this implies for our understanding of the *physical* causes of the evolution remains unclear.

The Very Large Array (VLA) of the National Radio Astronomy Observatory is operated by Associated Universities, Inc., under a cooperative agreement with the National Science Foundation. PG and MJK acknowledge PPARC support. Data reduction was partially carried out on STARLINK. We thank Steve Serjeant for useful conversations. We are grateful for the referee's comments which improved this paper.

REFERENCES

Bischof, O. & Becker, R.H., 1997, AJ, 113, 2000.

Blair M. & Gilmore G., 1982, PASP, 94, 742.

Boyle B.J., Staveley-Smith, L., Stewart, G.C., Georgantopoulos, I., Shanks T. & Griffiths, R.E., 1993, MNRAS, 265, 501.

Boyle B.J., Shanks T. & Peterson B.A., 1988, MNRAS, 235, 935.

Boyle B.J., Fong, R., Shanks T. & Peterson B.A., 1990, MNRAS, 243, 1.

Condon, J. et al., *preprint*, 1998, AJ.

Ellingson, E., Yee, H.F.C. & Green, R.F., 1991, ApJ, 371, 49.

Fitchett, M., 1988, MNRAS, 230, 161.

Goldschmidt P., Miller L., La Franca, F. & Cristiani, S., 1992, MNRAS, 256, 65p.

Goldschmidt P. & Miller L., 1998, MNRAS, 293, 107.

Goldschmidt P., 1993, Ph. D. thesis, University of Edinburgh.

Hazard, C., Mackay, M.B. & Shimmins, A.J., 1963, Nature, 197, 1037.

Hewett P.C., Foltz C.B. & Chaffee F.H., 1995, AJ, 109, 1498.

Hewett P.C., Foltz C.B. & Chaffee F.H., 1993, AJ, 406, L43.

Hooper, E. J., Impey, C.D., Foltz, C.B. & Hewett, P.C., 1995, ApJ, 445, 62. (HIFH)

Hooper, E. J., Impey, C.D., Foltz, C.B. & Hewett, P.C., 1995, ApJ, 473, 746.

Kellermann, K.I., Sramek, R., Schmidt, M., Shaffer, D.B. & Green, R., 1989, AJ, 98, 1195.

Koehler, T., Groote, D., Reimers, D. & Wisotzki, L., 1997, A&A, 325, 502.

La Franca, F., Cristiani, S., Barbieri, C., 1992, AJ, 103, 1062.

La Franca, F., Gregorini, L., Cristiani, S., de Ruiter, H. & Owen, F., 1994, AJ, 108, 1548.

McLeod, K.K. & Rieke, G., 1995, ApJ, 454, 77.

Marshall H.L., Avni Y., Braccesi A., Tananbaum H., Zamorani G. & Zitelli V., 1984, ApJ, 283, 50.

Miller, L., Goldschmidt, P., La Franca, F. & Cristiani, S., 1993, *Observational Cosmology ASP Conf. Series* 51, 614.

Miller, L., Peacock, J.A. & Mead, A.R.G., 1990, MNRAS, 244, 207. (MPM)

Miller, P., Rawlings, S. Saunders, R., 1993, MNRAS, 263, 425.

Osmer, P.S. & Smith, M.G., 1980, ApJS, 42, 333.

Peacock, J.A., Miller, L. & Longair, M.S., 1986, MNRAS, 218, 265.

Sandage, A., 1965, ApJ, 141, 1560.

Schmidt M., 1963, Nature, 197, 1040.

Schmidt M. & Green R.F., 1983, ApJ, 269, 352.

Schneider, D.P., Van Gorkom, J.H., Schmidt, M. & Gunn, J.E., 1992, AJ 103, 1451.

Serjeant, S.B.G., Rawlings, S., Maddox, S.J., Baker, J.C., Clements, D.C., Lacy, M. & Lilje, P.B., 1998, MNRAS, *in press*.

Smith, M.G. & Wright, A.E., 1980, MNRAS, 191, 871.

Stocke, J., Morris, S.L., Weymann, R.J. & Foltz, C.B., 1992, ApJ, 396, 487.

Strittmatter, P.A., Hill, P., Pauliny-Toth, I.I.K., Steppe, H. & Witzel, A., 1980, A & A, 88, L12.

Taylor, G.L., Dunlop, J.S., Hughes, D.H. & Robson, E.I., 1996, MNRAS, 283, 930.

Véron-Cetty, M.-P. & Woltjer, L., 1990, A & A, 228, 471.

Visnovsky, K., Impey, C.D., Foltz, C.B., Hewett, P.C., Weymann, R.J., Morris, S.L., 1992, ApJ, 391, 560.

White, R., Becker, R.H., Helfand, D.J., Gregg, M.D., 1997, *ApJ*, 475, 479.
Zitelli, V., Mignoli, M., Zamorani, G., Marano, B. & Boyle, B.J., 1992, *MNRAS*, 256, 349.

Fig. 1.— The optical luminosity-redshift plane, showing the distribution of quasars in optically-selected samples for which radio data was available prior to this paper, including the objects from the Palomar-Green (PG) Bright Quasar Survey.

Fig. 2.— Optically-selected quasar samples for which radio data is now available, including the new data described in this paper. For reasons outlined in the text, we have not included the BQS quasars. Note how the new data significantly extends the coverage of the $M_B - z$ plane.

Fig. 3.— The optical luminosities and redshifts of radio-loud and -quiet quasars from the samples used in this paper, showing the distribution of radio properties. Empty circles denote radio-quiet quasars, filled circles denote radio-louds.

Fig. 4.— The radio-luminosity - optical luminosity plane for quasars with $0.3 \leq z \leq 1.5$ used in this paper. Note that there is no evidence for a correlation between radio and optical luminosity for the quasars which have been detected in the radio, and also that the radio luminosity distribution appears to be bimodal.

Fig. 5.— The radio-luminosity - optical luminosity plane for quasars with $1.5 \leq z \leq 2.5$ used in this paper.

Fig. 6.— Fraction of radio-loud quasars as a function of redshift using data from this paper, together with the 2 parameter evolution model (solid line indicates best-fit, dashed lines indicate 1σ errors), and the no-evolution model (horizontal dot-dashed line). Also plotted is the fraction as determined from the PG sample in Kellerman et al. (1989).

Fig. 7.— Fraction of radio-loud quasars as a function of absolute magnitude in the redshift ranges $0.3 \leq z \leq 1.3$ and $1.3 < z \leq 2.5$ using data from this paper, the LBQS and MPM. The filled circles show the fraction of radio-louds in the lower redshift bin, and the empty circles show this fraction in the higher redshift bin. The error bars show the 1σ errors. Also shown is the model fit to the probability of a quasar being radio-loud as discussed in Section 6.

Fig. 8.— Results of Monte-Carlo simulation on the probability of a quasar being radio-loud as a function of absolute magnitude at $z = 1$. Note that although we assumed that the intrinsic distribution is constant with respect to M_B (horizontal line), the observed distribution rises with increasing luminosity.

Fig. 9.— The optical luminosity functions for radio-quiet quasars (dashed lines) and radio-loud quasars (solid lines), estimated from the derived likelihood of a quasar being radio-loud in Section 5.3. The lines are plotted for 4 different redshifts, from left to right: $z = 0.5, 1, 1.5, 2$.

Table 1. 5-GHz radio fluxes and positions for the Edinburgh quasars. Where no radio source was detected within 5" of the quasar's optical position we quote the optical position and the 3-sigma noise measured at the centre of the map as an upper limit to the flux density. Radio positions are accurate to 0.1". Colours, B magnitudes and redshifts are taken from Goldschmidt (1993). The 8.4 GHz flux from Hooper et al. (1995) is given in column 8 if the object has been included in that study. The symbol \dagger indicates that the quasar has already been detected by Parkes, MIT, Green Bank, Texas or Molonglo.

Object	RA (B1950)	Dec (B1950)	B	U-B	z	5 GHz flux (mJy)	8.4 GHz flux (mJy)
EQS B1228–0412	12 28 28.5	–04 12 02	18.1	–0.5	0.658	<0.3	
EQS B1228–0130	12 28 17.1	–01 30 31	18.0	–1.2	0.706	<0.3	
EQS B1229–0207 †	12 29 25.9	–02 07 32.0	17.8	–0.9	1.045	966.6	284.0
EQS B1230–0015 †	12 30 30.24	–00 15 01.7	17.7	–1.0	0.470	83.0	63.0
EQS B1235+0216	12 35 39.7	+02 16 48	18.2	–0.4	0.672	<0.235	<0.2
EQS B1236+0128	12 36 38.0	+01 28 42	18.0	–1.2	1.258	<0.3	<0.4
EQS B1237–0435	12 37 41.7	–04 35 03	18.4	–0.7	0.810	<0.3	
EQS B1237–0359	12 37 05.7	–03 59 22	17.9	–0.6	0.371	<0.3	
EQS B1237+0204	12 37 58.4	+02 04 44	17.7	–0.5	0.665	<0.2	<0.4
EQS B1240+0224	12 40 13.9	+02 24 43	17.9	–0.7	0.790	14.1	7.2
EQS B1242–0123	12 42 22.1	–01 23 10	18.1	–0.7	0.489	<0.1	<0.28
EQS B1243–0026	12 43 39.4	–00 26 10	17.1	–1.0	0.650	0.81	
EQS B1245–0333	12 45 00.4	–03 33 47	16.5	–0.9	0.379	<0.2	
EQS B1246–0430	12 46 17.0	–04 30 03	17.8	–0.9	0.531	<0.3	
EQS B1247–0213	12 47 13.2	–02 13 09	18.5	–1.0	1.312	<0.2	<0.3
EQS B1252+0200	12 52 46.4	+02 00 29	15.4	–1.4	0.345	0.80	
EQS B1253–0002	12 53 16.4	–00 02 17	17.7	–0.6	0.721	<0.2	
EQS B1254+0206	12 54 33.3	+02 06 52	17.3	–0.6	0.421	<0.3	
EQS B1255–0143	12 55 40.9	–01 43 08	17.7	–0.5	0.410	<0.2	
EQS B1257–0140	12 57 18.2	–01 40 58	17.7	–0.6	0.448	<0.2	
EQS B1303+0205 †	13 03 21.05	+02 05 32.3	17.1	–0.6	0.74	47.8	
	13 03 20.36	+02 05 11.0				40.07	
EQS B1305+0100	13 05 20.8	+01 00 22	17.8	–0.3	0.763	<0.2	
EQS B1305+0230	13 05 42.5	+02 30 10	17.2	–0.4	0.773	<0.2	
EQS B1306–0213	13 06 32.4	–02 13 18	17.6	–0.5	0.835	<0.3	
EQS B1308+0109 †	13 08 47.78	+01 09 15.2	17.9	–0.3	1.074	106.3	30.3
EQS B1311+0217	13 11 53.6	+02 17 07	17.1	–1.0	0.306	<0.3	<0.5
EQS B1313–0138	13 13 35.4	–01 38 15	17.9	–0.7	0.406	<0.3	<0.4
EQS B1315–0410	13 15 14.0	–04 10 14	17.7	–0.7	0.469	<0.2	
EQS B1315+0002	13 15 11.1	+00 02 56	18.1	–0.7	0.917	<0.2	
EQS B1315+0140	13 15 41.9	+01 40 37	18.1	–0.7	0.689	<0.2	0.34
EQS B1316–0734	13 16 48.4	–07 34 43	16.8	–0.7	0.538	<0.2	
EQS B1316+0023	13 16 06.5	+00 23 21	18.0	–0.7	0.490	<0.2	<0.3
EQS B1317–0033 †	13 17 04.70	–00 33 56.5	18.4	–0.8	890.0	678.7	
EQS B1319+0033	13 19 32.6	+00 33 40	18.1	–0.7	0.535	<0.2	<0.4

Table 1—Continued

Object	RA (B1950)	Dec (B1950)	B	U-B	z	5 GHz flux (mJy)	8.4 GHz flux (mJy)
EQS B1320-0006	13 20 49.9	-00 06 17	18.4	-0.5	1.388	<0.2	<0.4
EQS B1321-0549	13 21 38.68	-05 49 01.2	16.8	-0.6	0.732	29.3	
EQS B1324+0126	13 24 50.9	+01 26 55	18.3	-0.8	0.864	<0.2	
EQS B1328-0231	13 28 38.5	-02 31 46	18.7	-0.7	1.240	<0.2	
EQS B1328+0205	13 28 58.7	+02 05 12	18.2	-0.4	0.692	<0.2	<0.4
EQS B1329-0615	13 29 09.4	-06 15 21	17.6	-0.46	0.718	<0.2	
EQS B1329-0007	13 29 57.1	-00 07 55	18.3	-0.68	0.962	<0.2	
EQS B1334-0232	13 34 37.9	-02 32 37	17.7	-0.38	0.732	<0.3	<0.4
EQS B1334+0053	13 34 49.2	+00 53 27	18.3	-0.45	0.647	<0.2	<1.8
EQS B1335-0611 [†]	13 35 31.25	-06 11 56.8	17.8	-0.42	0.620	1021.8	
EQS B1335-0241	13 35 01.6	-02 41 54	18.0	-0.3	0.610	<0.2	<0.4
EQS B1335+0222 [†]	13 35 06.93	+02 22 12.5	18.0	-0.6	1.354	107.6	
EQS B1337-0146	13 37 17.0	-01 46 08	17.9	-0.5	1.010	<0.2	<0.2
EQS B1338-0030	13 38 10.4	-00 30 07	17.1	-0.6	0.389	<0.2	<0.3
EQS B1339-0648	13 39 49.7	-06 48 05	18.3	-0.9	1.220	<0.2	
EQS B1339-0526	13 39 41.4	-05 26 12	18.1	-0.5	1.252	<0.3	
EQS B1339-0459	13 39 39.3	-04 59 49	18.2	-0.8	0.884	<0.7	
EQS B1340-0020	13 40 12.2	-00 20 38	18.2	-0.6	0.792	<0.2	<0.4
EQS B1340+0107	13 40 25.8	+01 07 03	17.9	-0.7	1.067	<0.2	<0.3
EQS B1341-0357	13 41 34.4	-03 57 47	17.3	-0.8	0.835	<0.2	
EQS B1343-0607	13 43 23.7	-06 07 44	17.7	-0.7	1.012	<0.2	
EQS B1343-0221	13 43 13.1	-02 21 55	18.2	-0.3	0.509	<0.2	0.7
EQS B1344-0227	13 44 38.1	-02 27 36	18.2	-0.4	0.511	<0.2	<0.4
EQS B1345-0000	13 45 17.8	-00 00 23	18.0	-0.4	0.552	<0.2	<0.5
EQS B1346+0007	13 46 48.3	+00 07 55	18.3	-0.2	1.127	<0.2	<0.2
EQS B1347-0026	13 47 00.2	-00 26 11	17.6	-0.4	0.515	<0.2	<0.3
EQS B1348+0118	13 48 55.1	+01 18 28	17.7	-0.7	1.094	<0.2	<0.3
EQS B1349+0057	13 49 59.2	+00 57 39	18.0	-0.8	1.151	<0.3	<0.3
EQS B1352-0043	13 52 51.4	-00 43 00	18.4	-0.8	0.900	<0.3	
EQS B1354-0233	13 54 53.8	-02 33 03	17.1	-0.6	0.559	<0.6	
EQS B1354+0117	13 54 17.2	+01 17 22	17.9	-0.8	1.210	<1.5	
EQS B1357-0227	13 57 31.4	-02 27 02	17.6	-0.7	0.418	<0.3	
EQS B1358+0058	13 58 31.6	+00 58 01	17.5	-0.6	0.664	1.0	
EQS B1403-0304	14 03 35.2	-03 04 56	17.2	-0.8	0.860	<0.2	
EQS B1406-0143	14 06 54.15	-01 43 08.8	17.7	-0.7	0.644	72.4	
EQS B1407-0722	14 07 52.80	-07 22 32	18.1	-0.9	0.900	<0.2	
EQS B1407-0231	14 07 20.92	-02 31 56.7	17.9	-0.7	1.263	43.9	
	14 07 24.20	-02 31 24.4				29.0	

Table 1—Continued

Object	RA (B1950)	Dec (B1950)	B	U-B	z	5 GHz flux (mJy)	8.4 GHz flux (mJy)
EQS B1411–0333	14 11 41.4	–03 33 47	17.9	–0.5	0.860	<0.2	
EQS B1413+0107	14 13 16.6	+01 07 51	17.4	–0.6	1.042	<0.2	
EQS B1414–0544	14 14 30.8	–05 44 46	17.5	–0.6	0.419	<0.3	
EQS B1416–0518	14 16 33.6	–05 18 59	18.5	–0.7	0.96	13.1	
EQS B1420–0053	14 20 05.9	–00 53 09	17.7	–0.5	0.717	<0.3	
EQS B1421–0407	14 21 33.4	–04 07 42	18.1	–0.4	0.650	<0.2	
EQS B1421+0108	14 21 57.3	+01 08 32	18.1	–0.7	1.060	<0.3	
EQS B1423–0013	14 23 26.2	–00 13 31	17.9	–0.6	1.078	<0.3	
EQS B1424–0007	14 24 24.6	–00 07 30	16.5	–0.5	0.632	<0.3	
EQS B1429–0100	14 29 07.3	–01 00 17	17.4	–0.7	0.661	<0.2	<0.4
EQS B1429–0036	14 29 09.4	–00 36 58	18.5	–0.7	1.179	<0.4	<0.8
EQS B1430–0046 [†]	14 30 10.0	–00 46 04	17.7	–0.8	1.0	22.9	15.0
	14 30 11.1	–00 46 18				14.0	
	14 30 09.1	–00 45 53				20.6	
EQS B1437–0143	14 37 46.8	–01 43 37	18.3	–0.6	0.718	<0.2	<0.5
EQS B1440–0234	14 40 38.4	–02 34 40	17.4	–0.7	0.675	<0.3	<0.3
EQS B1440+0149	14 40 18.0	+01 49 38	18.2	–0.8	1.170	<0.2	<0.5
EQS B1446+0218	14 46 05.7	+02 18 54	18.1	–0.5	0.668	<0.2	<0.4

RA (1950)	Dec (1950)	<i>B</i>	<i>z</i>	S_ν	Offset
00 51 38	–27 26 25	18.9	0.689	6.5	3.3
00 49 28	–28 12 36	20.1	1.145	5.9	1.7
22 03 26	–18 50 17	19.0	0.620	6398.9	2.1
22 37 43	–39 18 35	19.1	0.713	2.4	4.7

Table 2: Table of quasars from AAT survey (Boyle et al., 1990) which have been detected in the NVSS (Condon et al., 1998). We present the 1950 coordinates of the optical position, the optical magnitudes, and radio fluxes in mJy, and lastly the offset between the optical and radio positions in arcseconds.

Table 2: Table of quasars from the LBQS survey (Hewett et al., 1995) which have been detected in FIRST (White et al., 1997). We present the B1950 coordinates of the optical position, the optical magnitudes (in B Johnson), and radio fluxes in mJy, and lastly the offset between the optical and radio positions in arcsecs.

RA (1950)	Dec (1950)	<i>B</i>	<i>z</i>	S_ν	Offset
00 02 33	−01 49 28	18.8	1.709	63.9	0.9
00 04 36	+00 36 46	17.9	0.316	1.4	1.2
00 09 41	−01 48 10	17.8	1.072	1.1	0.1
00 12 10	−00 16 59	18.3	1.524	1.5	1.3
00 12 33	−00 24 42	18.7	1.701	13.5	0.7
00 19 07	+00 22 03	18.7	0.313	1.4	0.4
00 20 11	−02 02 29	18.4	0.691	214.8	0.3
00 21 38	−01 00 25	18.2	0.764	1.0	1.0
00 24 44	+00 20 47	18.0	1.228	3.7	1.5
00 29 03	−01 52 56	18.7	2.382	14.1	0.1
00 48 57	+00 25 32	18.2	1.187	13.8	1.0
00 49 32	+00 19 21	16.5	0.397	88.0	1.0
00 52 07	−00 15 04	17.8	0.647	2.7	0.4
00 56 32	−00 09 19	17.8	0.717	2416.0	0.3
00 59 32	−02 06 46	18.1	1.320	1.8	0.5
01 07 40	−02 35 51	18.2	0.957	188.5	3.0
02 49 22	+00 44 50	18.5	0.469	8.1	0.7
02 51 07	−00 01 02	18.4	1.682	7.6	1.1
02 56 06	−02 06 08	18.5	0.406	1.1	1.4
02 56 32	−00 00 34	18.3	3.363	2.6	1.4
02 56 55	−00 31 54	17.7	1.995	225.0	0.5
02 57 03	+00 25 42	16.9	0.531	0.8	0.1
22 31 26	−00 48 46	17.6	1.209	1.0	1.5
22 35 01	+00 54 58	18.6	0.528	1.1	1.0
22 45 05	−00 55 44	17.5	0.800	1.6	1.8
23 51 35	−00 36 30	18.5	0.460	346.1	0.6
23 59 16	−02 16 23	18.8	2.816	25.0	6.3
23 59 49	−00 21 26	18.6	0.809	3.9	0.9

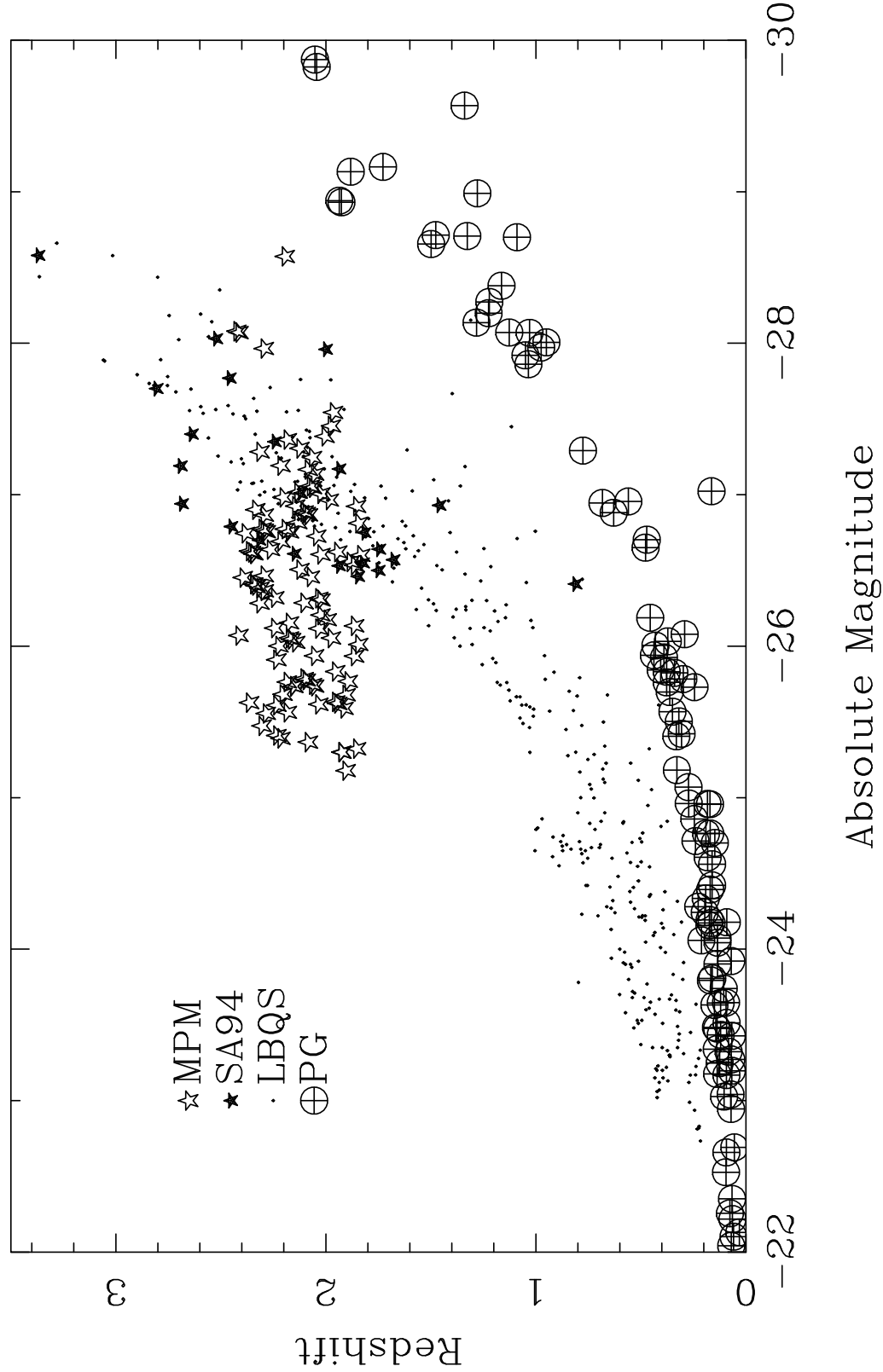


Figure 1

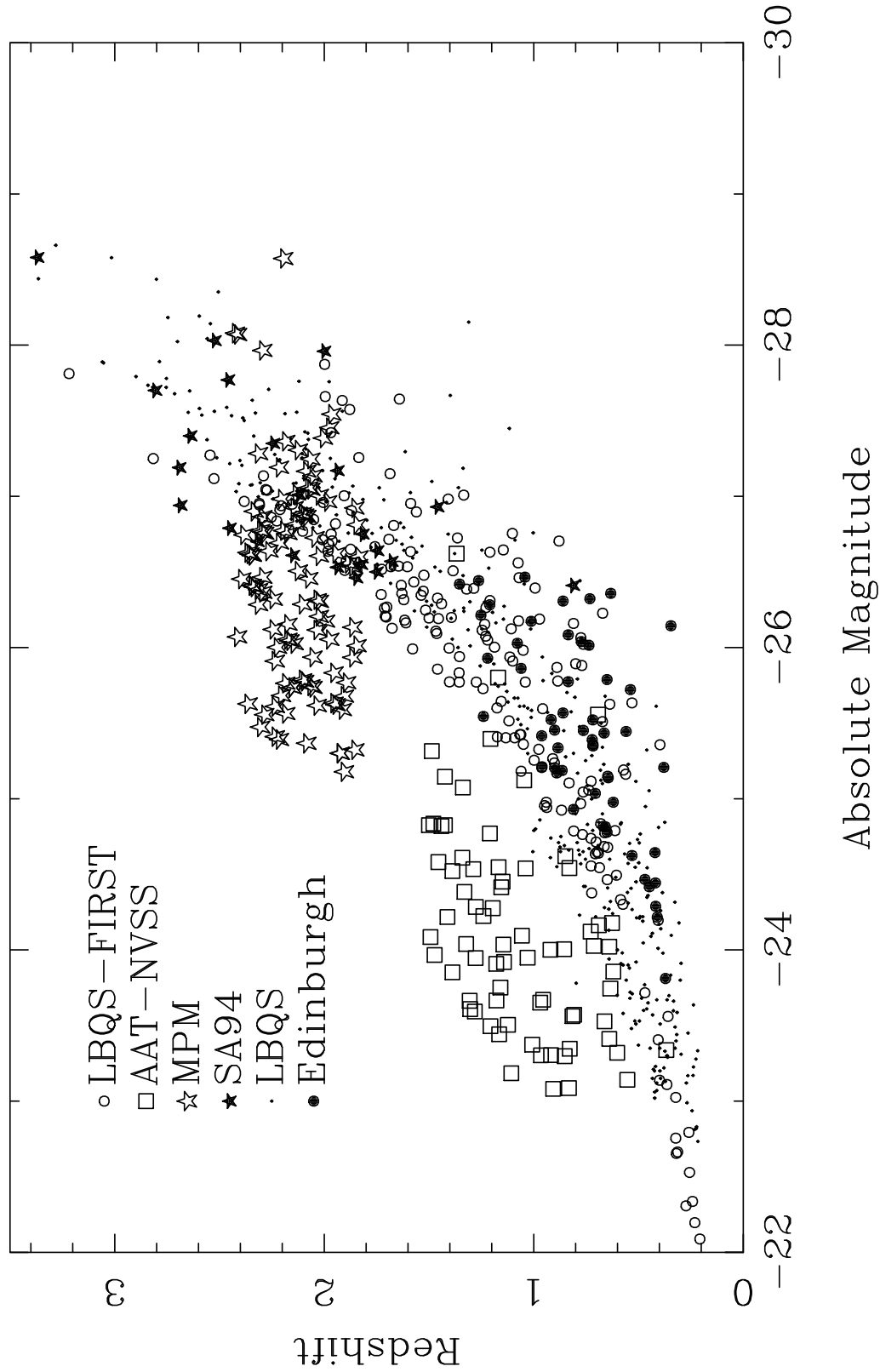


Figure 2

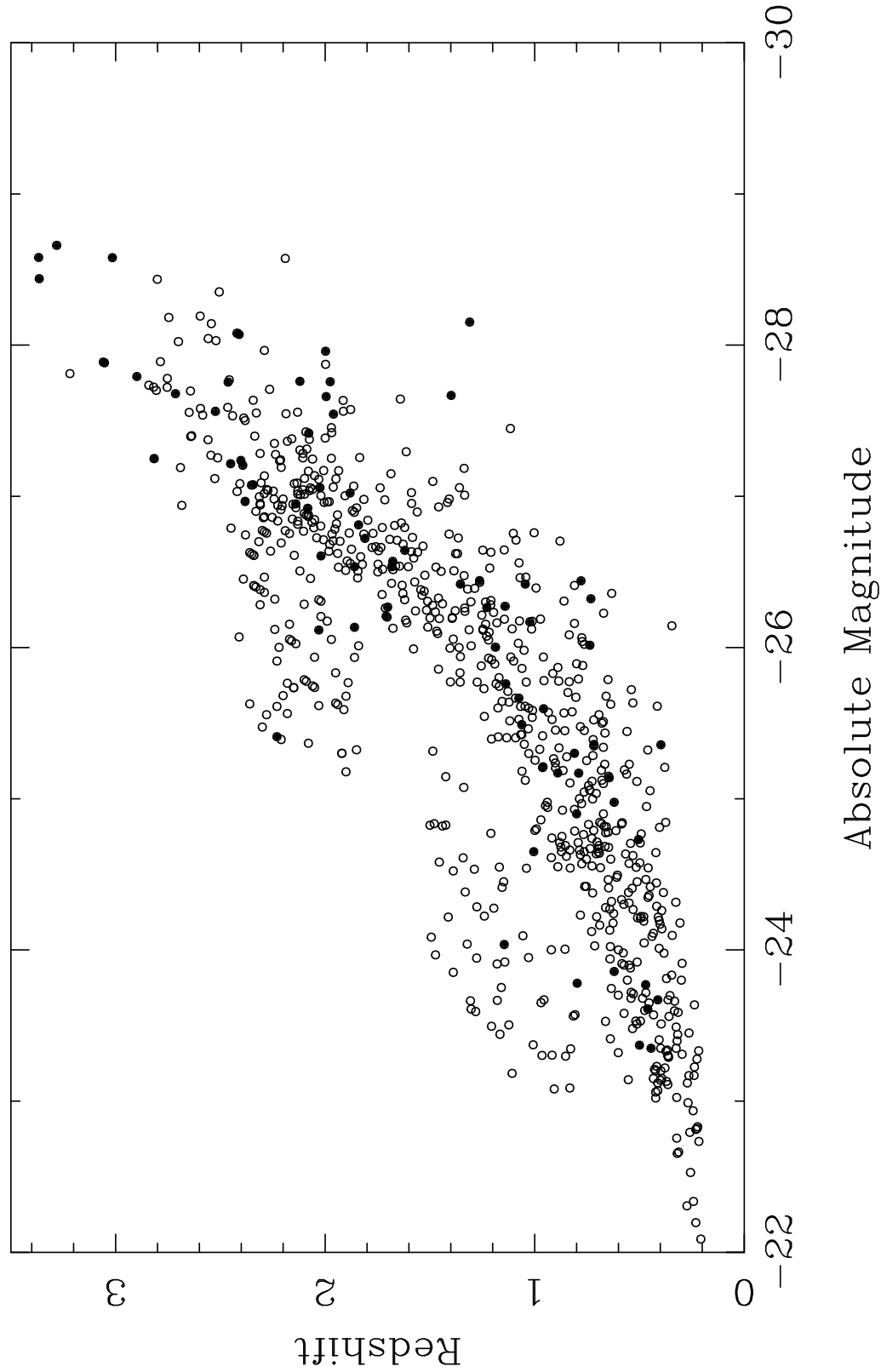


Figure 3

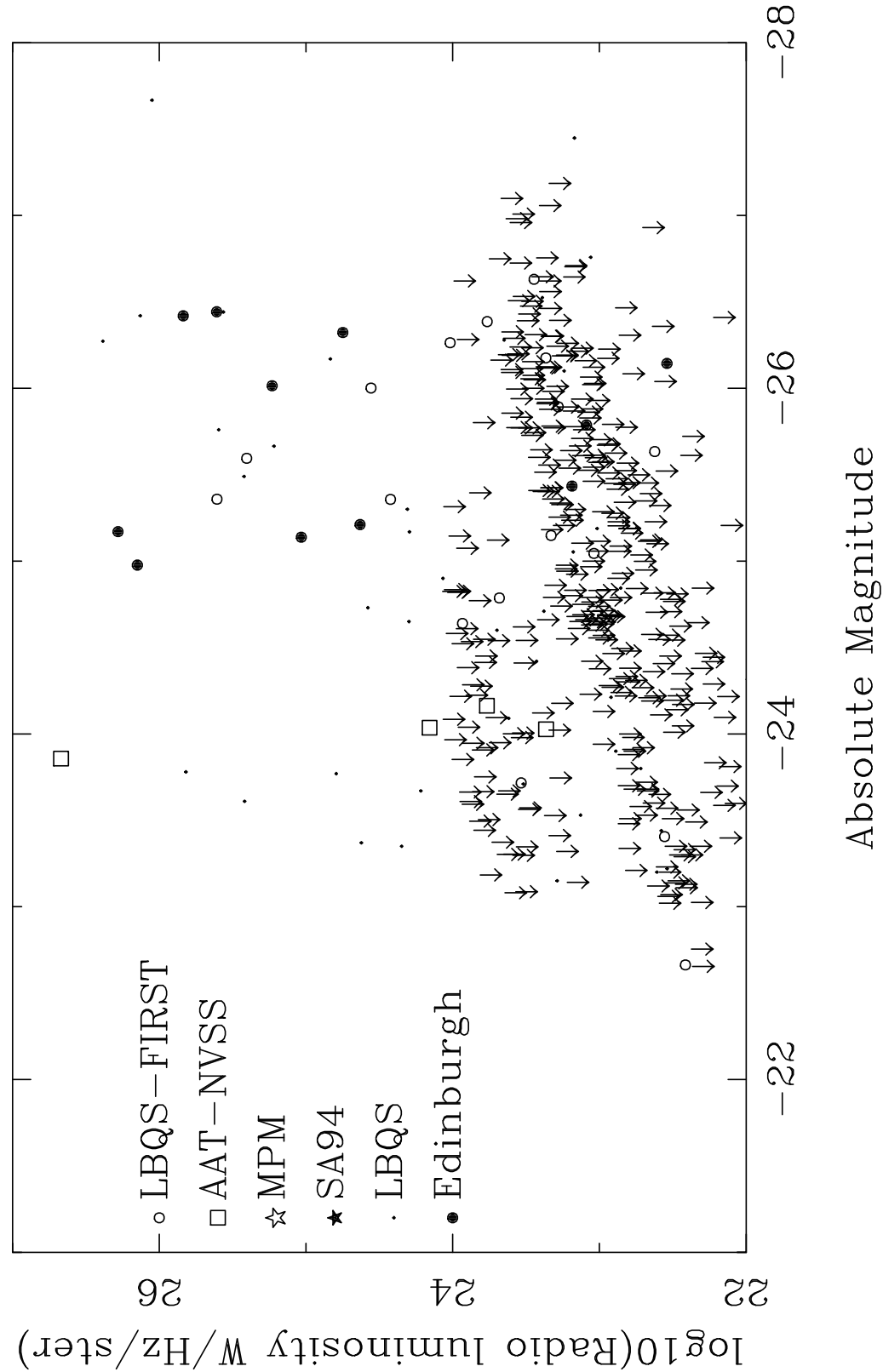


Figure 4

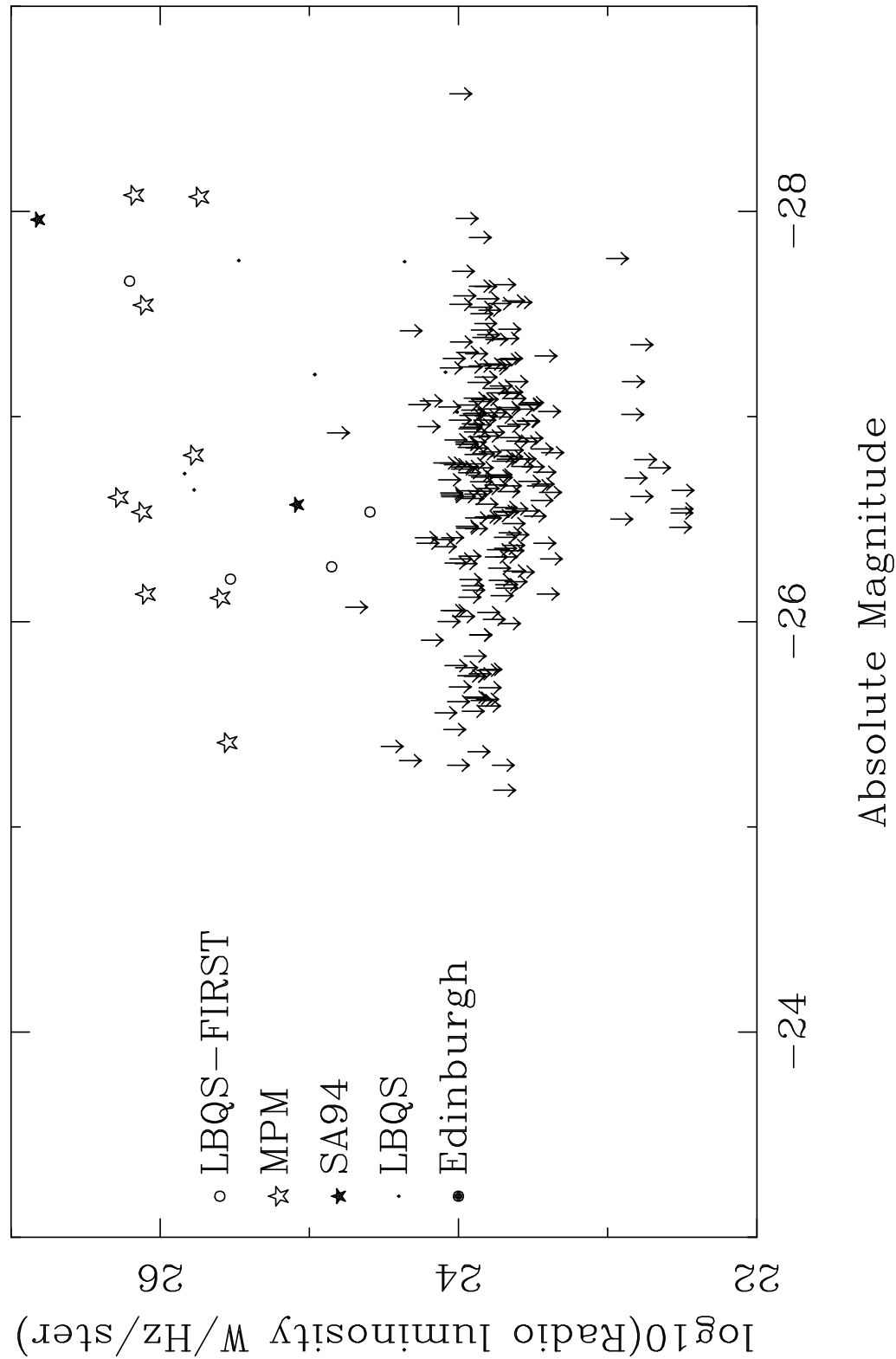


Figure 5

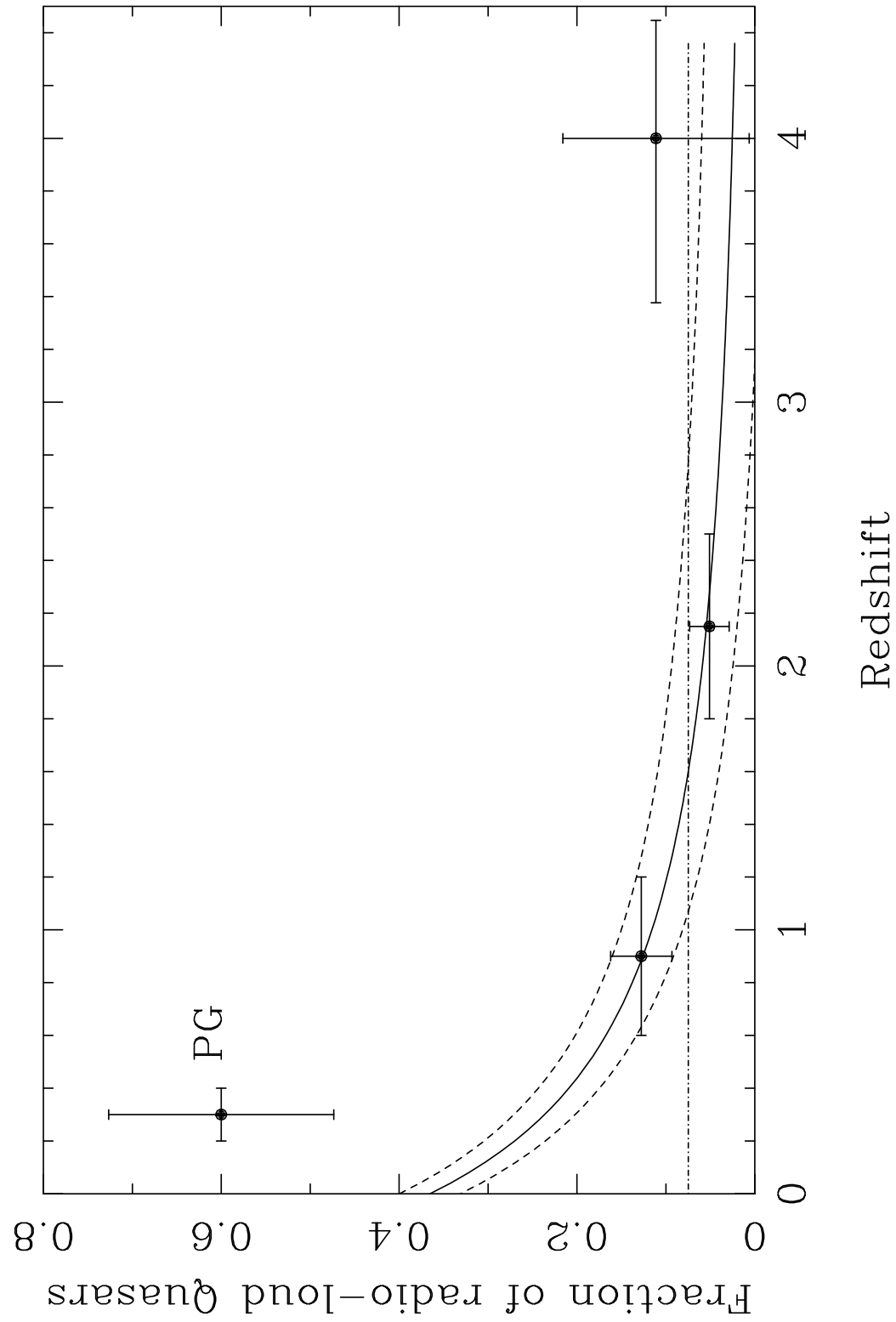


Figure 6

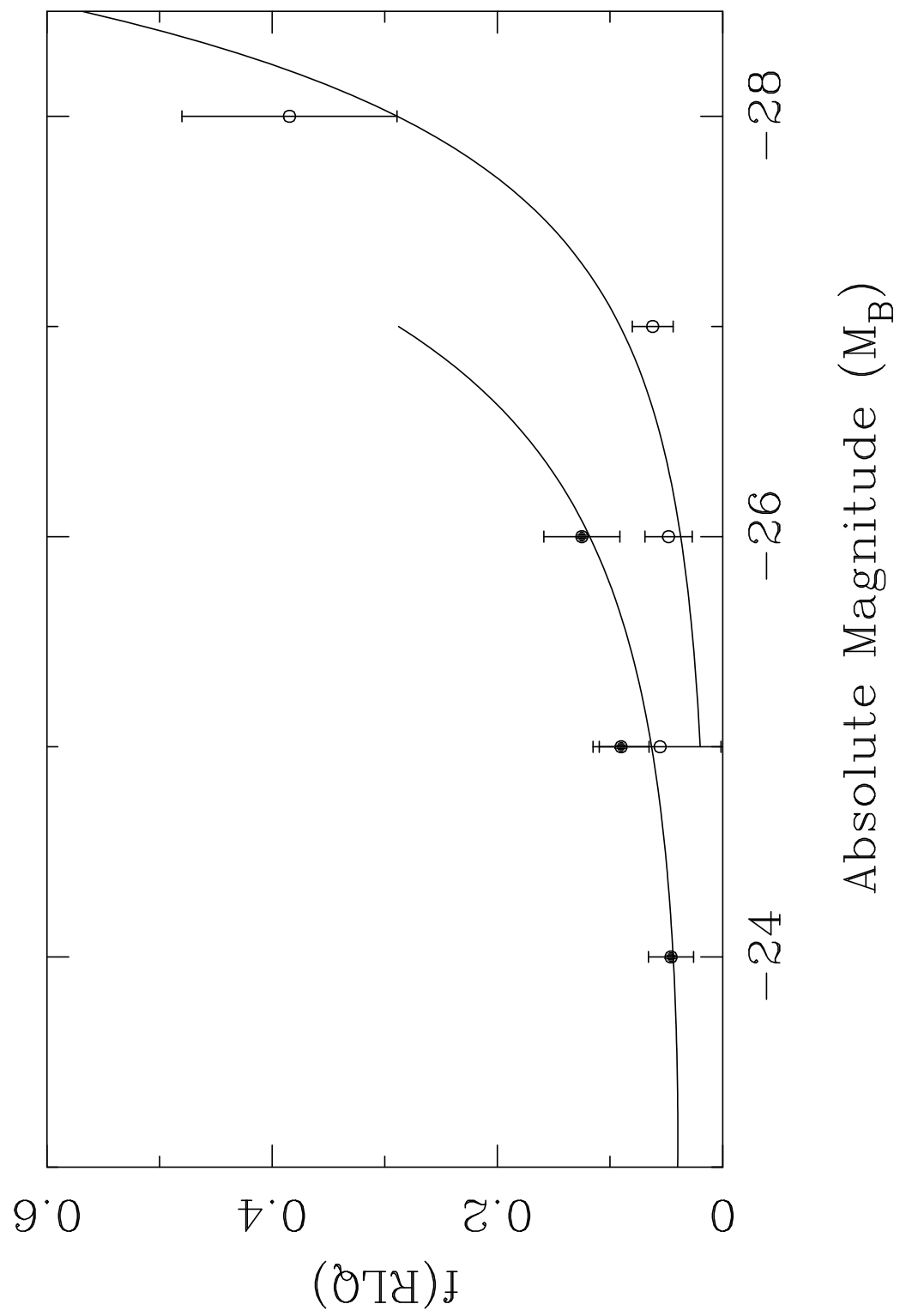


Figure 7

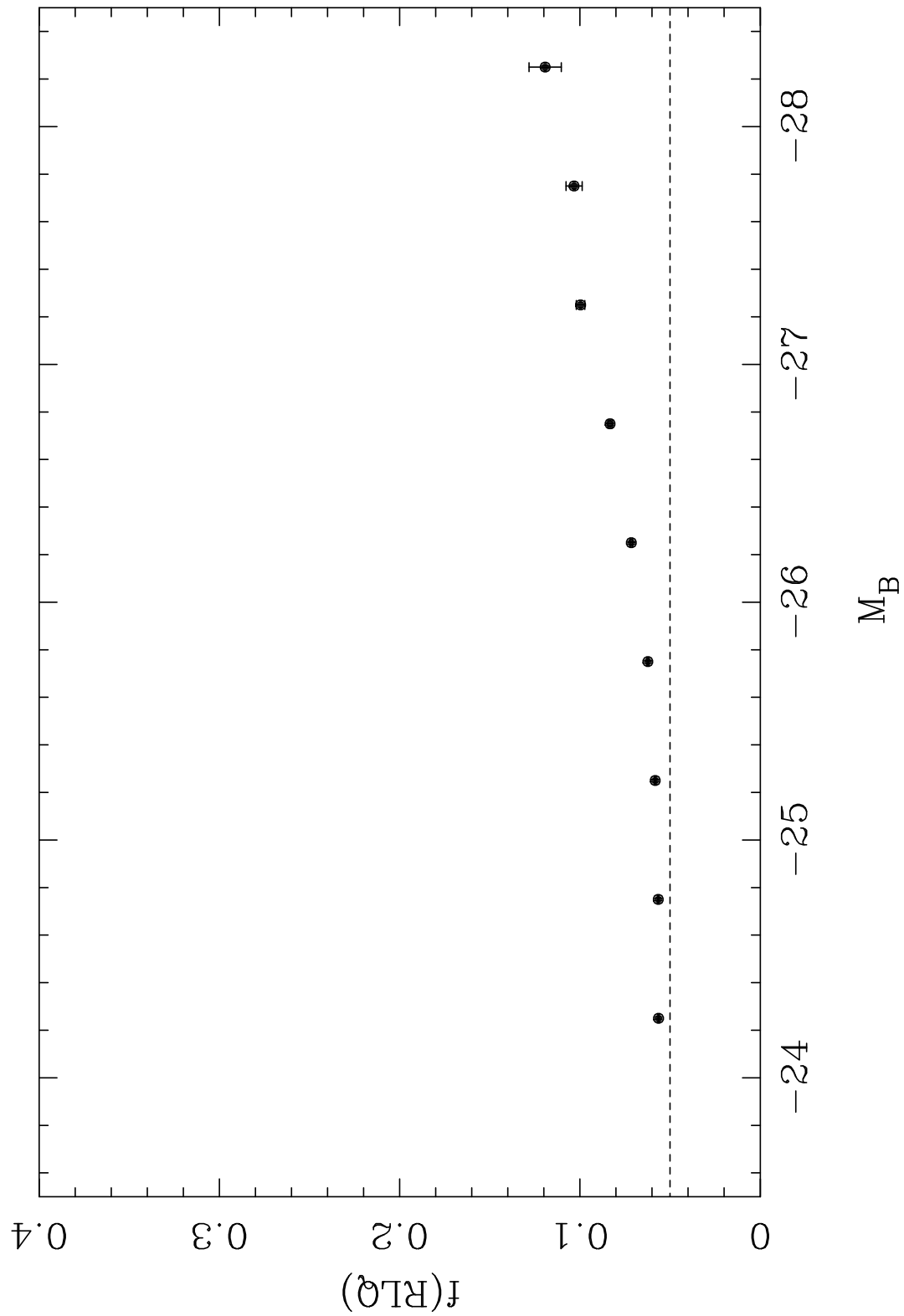


Figure 8

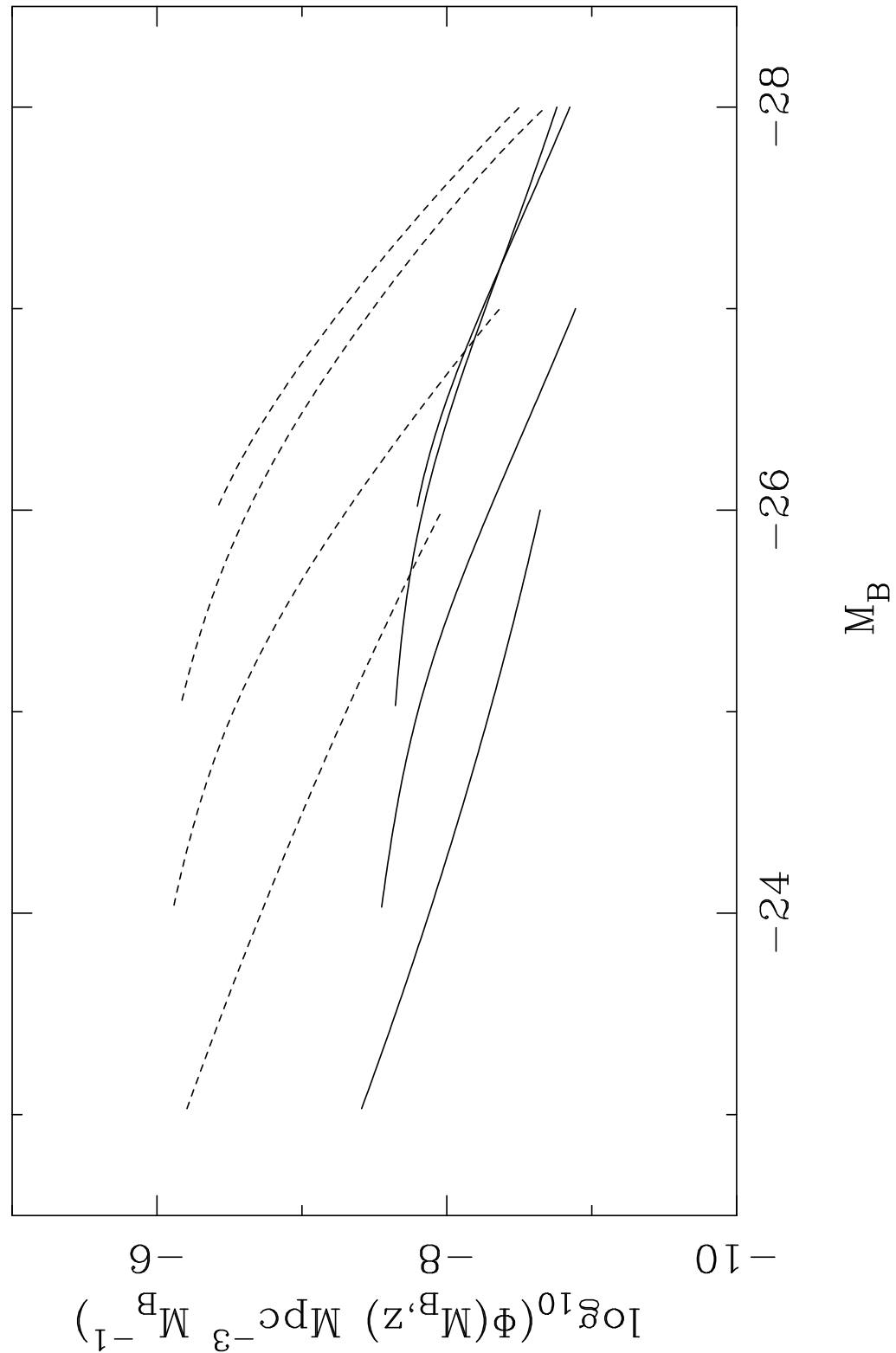


Figure 9